Journal of Food Engineering 117 (2013) 217–226

Contents lists available at SciVerse ScienceDirect

Journal of Food Engineering

journal homepage: www.elsevier.com/locate/jfoodeng

Use of a portable hyperspectral imaging system for monitoring the efficacy of sanitation procedures in produce processing plants

Michael S. Wiederoder [a,b], Nancy (Tong) Liu [a,b], Alan M. Lefcourt [a,*], Moon S. Kim [a], Y. Martin Lo [b]

[a] USDA, Agricultural Research Service, Environmental Microbial and Food Safety Laboratory, Bldg. 303, Beltsville, MD 20705, USA
[b] Department of Nutrition and Food Science, University of Maryland, College Park, MD 20740, USA

a r t i c l e i n f o

Article history:
Received 3 October 2012
Received in revised form 8 February 2013
Accepted 11 February 2013
Available online 26 February 2013

Keywords:
Hyperspectral imaging
Food safety
Sanitation inspection
Portable
Produce

a b s t r a c t

Cleaning and sanitation of production surfaces and equipment plays a critical role in lowering the risk of food borne illness associated with consumption of fresh-cut produce. Visual observation and sampling methods including ATP tests and cell culturing are commonly used to monitor the effectiveness of the cleaning procedures. This study tested the ability of a hand-held VIS hyperspectral imaging system to augment current monitoring methods. Multiple visits were made to two commercial fresh-cut processing facilities. Fluorescence-based detection and automated cycling among three wavelengths, 475, 520, and 675 nm, proved best for detecting a range of anomalies. Numerous deficiencies in existing cleaning protocols were identified. Plant personnel were able to devise changes in the protocols that eliminated most of the detected problems without increasing the net expenditure for cleaning efforts. In addition, imaging identified sites where ATP test results were higher when compared to results for adjacent areas.

Published by Elsevier Ltd.

1. Introduction

An estimated 48 million cases of foodborne illness occur annually in the United States with 29.4% of these illnesses deriving from produce and associated products (Scallan et al., 2011; Hoffmann et al., 2007). Between 1996 and 2006, 72 foodborne illness outbreaks were associated with fresh produce consumption with 18 of these connected to fresh-cut produce (FDA, 2008). For fresh produce, the principal factor responsible for the increased relative risk of foodborne illness compared to other foods is the absence of a lethal process (e.g., heat) prior to consumption. Other factors that contribute to the increased risk include handling and mixing of large product volumes, damage to natural protection barriers, high environmental moisture and nutrient content, and temperature abuse during transport, processing, storage, or retail display (FDA, 2001). To minimize the effects of these factors, two strategies commonly employed are refrigeration and implementation of a General Hygiene Plan (GHP). Refrigeration is used to keep the produce below a temperature threshold at all times; thus, reducing the risk of microbial growth. A GHP requires a cleaning and sanitation program designed to remove contaminants from food contact surfaces. In addition to reducing the potential for direct transfer of organisms, contamination removal reduces the risk of biofilm formation. Biofilms that are resistant to cleaning and sanitation can provide safe havens for pathogens and spoilage microorganisms (Kumar and Anand, 1998; Donlan and Costerton, 2002; Fatemi and Frank, 1999), and be a source for cross contamination events by releasing these organisms back into the surrounding environment (Poulsen, 1999; Silagyi et al., 2009). Current industry methods used to verify surface hygiene after cleaning and sanitation include visual inspection with the naked eye, adenosine triphosphate (ATP) bioluminescent assays, and culturing techniques. However, ATP tests and culturing techniques require sub-sampling of surfaces, disposable reagents, expert personnel, and a variable wait time (5–15 min for ATP tests and 24–48 h for culturing; Pérez-Rodríguez et al., 2008). Furthermore, the limited locations sampled probably do not reflect real-time plant conditions (Lammerding and Frazil, 2000). A need exists for a method that can detect contaminants in real-time over large surface areas with greater sensitivity than visual inspection with the naked eye.

In this study, the potential for using a hand-held imaging system to detect contaminants following cleaning and sanitation at two commercial fresh-cut processing plants is explored. The imaging device used is a hyperspectral system capable of acquiring images or movies at visible wavelengths; an integral violet LED illumination source allows acquisition of fluorescence as well as reflectance data (Lefcourt et al., 2013). Studies have demonstrated that fluorescence imaging can detect produce processing residues (Wiederoder et al., 2012) and biofilms (Jun et al., 2009, 2010) at multiple wavelengths. Additionally, many organic compounds fluoresce when subject to UV excitation, including, chlorophyll-a

* Corresponding author. Tel.: +1 301 504 8450x258; fax: +1 301 504 9466.
E-mail address: alan.lefcourt@ars.usda.gov (A.M. Lefcourt).

0260-8774/$ - see front matter Published by Elsevier Ltd.
http://dx.doi.org/10.1016/j.jfoodeng.2013.02.019

at 670–680 nm (Brody, 1958), lignins and other phenolics at blue wavebands (Fry, 1979, 1982; Lundquist et al., 1978), and vitamin K, reduced nicotinamide adenine dinucleotide (NADPH), beta-carotene, and riboflavin with maxima at 420, 440, 490, and 525 nm respectively (Chappelle et al., 1991). Methods used to investigate the validity of detected anomalies include immediate re-cleaning and ATP testing.

2. Materials and methods

2.1. Imaging system

The imaging system, including operating characteristics and criteria used to select detection wavelengths, has been described in detail (Lefcourt et al., 2013; Fig. 1). The camera head incorporates a 12-bit charge coupled device (CCD) camera (Prosilica GC1380, Allied Vision Technologies, Germany), a liquid crystal tunable filter (400–720 nm, 20 nm FWHM; VariSpec VIS, Caliper Life Sciences, USA), back-correction optics (Channel Systems, Canada), and a C-mount lens (Rainbow S16mm, 2/3″, Sensei Shoj Co., Japan). Four 405-nm light emitting diodes (LED's) (LZ4-40UA10, LED Engin., Inc., Santa Clara, CA) provide illumination for fluorescence excitation, and a touchscreen monitor (7″; 705TSV, Xenarc Technologies Corp., USA) allows for real-time display and parameter selection, and offline analyses. The camera head includes a pistol grip (AF2100, Silk, Japan) that allows use with or without a tripod (3021BPro, Manfrotto Distribution Inc., USA), and is tethered to a backpack containing rechargeable lithium-ion batteries (18V, 10 AH; ONLYBATTERYPACKS, USA), a laptop computer (D430, Dell, USA), and the filter controller.

2.2. ATP bioluminescence measurement

To estimate surface ATP concentration, a swab (PocketSwab Plus, Charm Sciences Inc., Lawrence, MA) was stroked 3 times in a "Z" pattern over a surface area of approximately 400 cm^2. The swab was then activated and the fluorescence response measured using a luminometer (novaLUM, Charm Sciences Inc.), which displayed responses in relative light units (RLUs).

Fig. 1. Portable hyperspectral imaging system including monitor, violet LEDs, and tripod used for acquiring hyperspectral image data.

2.3. Produce plants

Multiple trips to fresh-cut processing Plant A were made in 2010 and 2011; four trips were made to Plant B in 2011. Measurements were made after completion of the daily cleaning and sanitation procedures that occurred prior to the start of production. Plant A's procedure was to wash, rinse, and then sanitize a limited area starting at one side of the facility and proceeding in a stepwise fashion across the facility. Plant B's procedure was similar, except each cleaning step was completed for the entire facility before proceeding to the next step.

2.3.1. Imaging

Images were binned by three in both dimensions to yield an effective resolution of 453 (H) × 341 (V) pixels, and were displayed at 15 frames per s at either 610 nm with LED illumination off or while cycling through three wavelengths (475, 520, and 675 nm) at one s intervals with LED illumination on. Cycling could be stopped and restarted by tapping on the monitor screen. The three cycled wavelengths were chosen in part to take advantage of the variability of the intensity of fluorescent lighting as a function of wavelength. The imaging system includes an automate routine that sets the camera gain as a function of wavelength (Fig. 2; Lefcourt et al., 2013). The three cycled wavelengths correspond to regions of high gain (i.e., low illumination intensity) in the facilities environments, while 610 nm corresponds to a region of low gain. The low ambient illumination intensities at the cycled wavelengths reduced the potential for ambient lighting to mask fluorescence responses to LED illumination. Because of the high illumination intensity at 610 nm acquired images have the appearance of "normal" monochrome pictures, which allowed the images to be used to identify the surface being examined.

Once a potential anomaly was detected, a hyperspectral data cube was acquired from 460 to 720 nm at 5 nm increments with and then without LED illumination. The acquired data allowed calculation and sequential display of difference images using a selectable dwell time. The subtraction procedure was done to negate the effects of ambient illumination and, thus, to emphasize fluorescent responses. Total elapsed time for the entire sequence of events was normally around 30 s. To document acquisitions, a digital camera (PowerShot G9, Canon, Lake Success, NY) was used to capture a photograph of the surface area of interest as well as a wide angle shot to document the camera's orientation and distance relative to the point of interest. For each anomaly, written notation was made of time, surface location, surface type, surface function, samples taken, and visual observations.

2.3.2. Plant procedures

Because of the limited time period between end of cleaning and start of production, it was impossible to do a complete survey of an

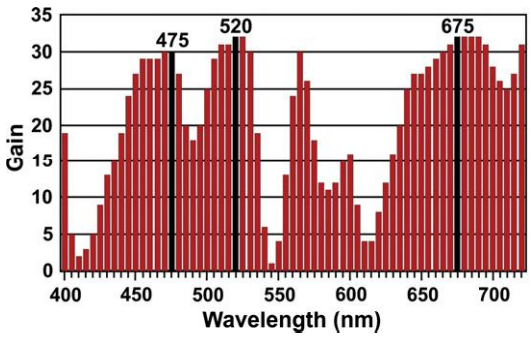

Fig. 2. Typical profile of camera gain by wavelength. The gains at the three wavelengths used for cycling occurred at local gain maxima, which correspond to lower ambient light intensities.

entire facility during a single visit. For each visit, a set of goals was established on arrival after talking with onsite personnel. While goals were being addressed, one member of the team would talk with onsite personnel and scout the facility for potential problems areas, which would then be investigated if time allowed. After all visits, images were cataloged and annotated copies of the most interesting images were emailed to the company contact along with any ancillary notes or ATP test results.

When a site was selected for investigation, an attempt was made to characterize the source of the detected anomaly. In many cases, the source could be identified visually or could be classified as conforming to the characteristics of a known category of problems. Based on this identification process, a decision was made as to whether to initiate ATP testing. Tests were always conducted by a company employee who swabbed the area indicated by the person doing the imaging. If this test resulted in a reading of concern, then additional tests were made in areas adjacent to, but outside, the anomalous area to allow comparison with initial test results.

3. Results and discussion

The sources of detected anomalies could be grouped into three categories: produce residues, blemishes in surface structures, and a less well defined group encompassing stains, biofilms, and localized build-up or accumulation of substances. Produce residues were visible at 675 nm and were sometimes visible at other wavelengths. Most particulate residues could be identified by eye after detection; however, it is unlikely they would have been noticed without the help of the imaging system. Juice from produce was detected and was seldom visible to the naked eye.

The most commonly detected anomalies in surface structures involved HDPE and were visible at 475 and 520 nm. Sources of detected anomalies included wear in conveyer belts, knife cuts, and alterations made during fabrication or modification, e.g. drilling. Occasionally, welds and bends in metal structures were detected; speculated to be due to surface roughness.

3.1. Examples of produce residues

3.1.1. Plant A – diced celery

Images were acquired of a conveyer belt last used to transport diced celery after completion of normal cleaning and sanitation procedures. Fig. 3 shows a photograph and a 675 nm image acquired at a distance of about 1–2 m from the equipment. Fluorescence-based responses to the violet LED illumination clearly identified celery pieces not easily visible to the naked eye. Further examination determined that celery pieces had settled into crevices where belt sections join, making them difficult to remove by normal cleaning and sanitation procedures. The company successfully re-cleaned the belt prior to the beginning of production.

3.1.2. Plant A – potato debris

Visual inspection of the potato peeler was made difficult by poor lighting within the unit and it was almost impossible to see the potato particulates hidden in the white brushes with the naked eye. Fluorescence-based responses of the particulates were seen at multiple wavebands: 510–530, 550–570 and 660–690 nm. Of the three cycling wavelengths, the 520 nm wavelength provided the best sensitivity for detection (Fig. 4). Employees of Plant A immediately re-cleaned the peeler and modified the existing procedure to include spraying cleaning and sanitation solutions from multiple angles to better remove debris. Similar results were seen when carrot peeling equipment were imaged.

3.1.3. Plant B – onion debris

Small onion particulates barely visible to the naked eye were found in crevices in the blue plastic transport belt (Fig. 5). After scanning nearby equipment, it became evident that there was an unusually high incidence of produce particulates on equipment. It turned out that the normal cleaning crew of five had been reduced to three due to illnesses. Immediate steps were taken to remedy the identified problems, and procedures were established to deal with short staff situations. The ability to quickly detect this change in relative cleanliness due to a manpower shortage suggests that the imaging system can be used to monitor routine cleaning efforts.

3.2. Examples of surface structures

3.2.1. Cutting boards

HDPE cutting boards are ubiquitous in both Plants A and B. Fluorescent anomalies for these materials appeared to be due to accumulated chemical residues, or damage to or imperfections in physical structure. Fig. 6 shows a vegetable cutting board from in Plant B; the distinct area of fluorescence found at 675 nm is indicative of chlorophyll-a related compounds as the response was only seen in wavelengths around 675 nm.

ATP tests were conducted for the fluorescent area and an area nearby. Measured responses for both test areas (Table 1) exceeded

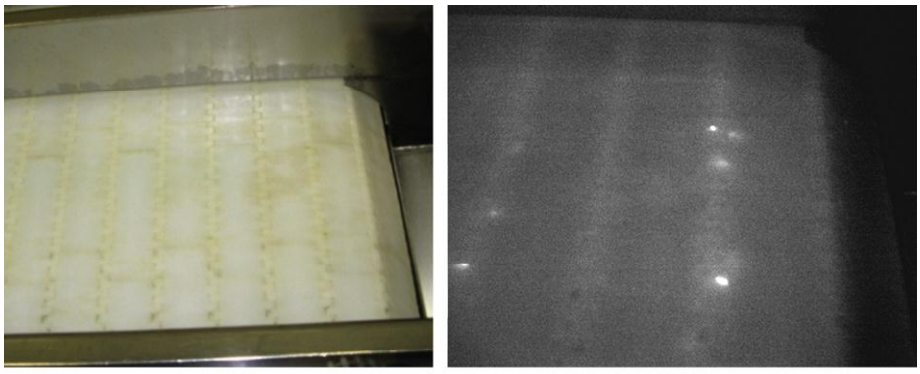

Fig. 3. Images of a celery sorting belt in Plant A. Digital photograph (a) and image at 675 nm with violet LED illumination (b) were acquired after cleaning and sanitation. The bright white dots in (b) are pieces of celery.

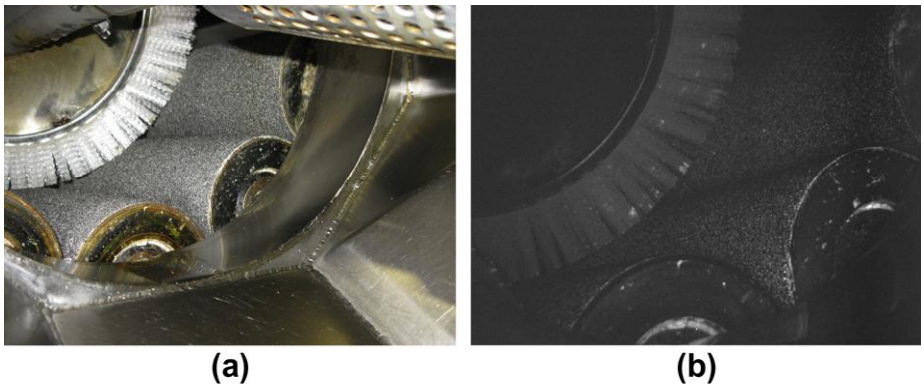

Fig. 4. Industrial potato peeler in Plant A. Digital photograph (a) and image at 520 nm with violet LED illumination (b) were acquired after cleaning and sanitation. The white spots in the brushes are potato particulates; the white ring around rollers is accentuated by the presence of fluorescent grease used for lubrication.

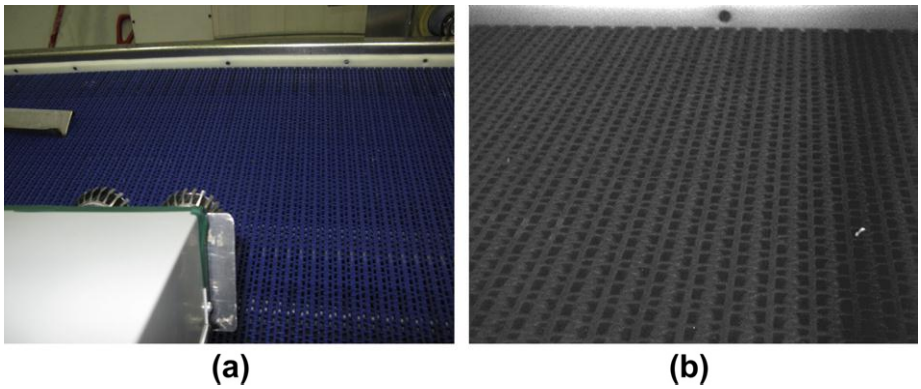

Fig. 5. Onion transport belt in Plant B. Digital photograph (a) and image at 675 nm with violet LED illumination (b) were acquired after cleaning and sanitation.

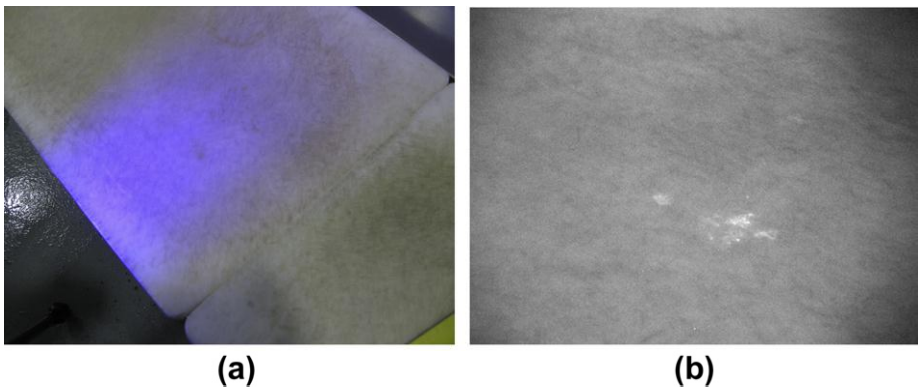

Fig. 6. Vegetable cutting board (HDPE) in Plant B. Digital photograph (a) and image at 675 nm with violet LED illumination (b) were acquired after cleaning and sanitation.

acceptable limits (~100 RLU). These results were interpreted to indicate that the cutting board had not been adequately cleaned. Plant B employees immediately re-cleaned the board, and decided to specifically monitor the cleanliness of cutting boards as part of routine cleaning procedures.

In another case, extensive damage near the edge of a cutting board was detected using fluorescence-based responses at 475 and 520 nm (Fig. 7). There was no anomalous fluorescence response at 675 nm. ATP tests were taken of the fluorescent area and a non-fluorescent area nearby (Table 2). The readings for the damaged area were much greater than for an area adjacent to the damaged area. A similar edge problem was observed in Plant B (Fig. 8). Similar trends in ATP results were also observed (Table 3).

Table 1
ATP test results for cutting board shown in Fig. 6.

ATP test location	ATP result (RLU)
Yellowish/brown fluorescent stain	34,713
Nearby white area of cutting board	176,559

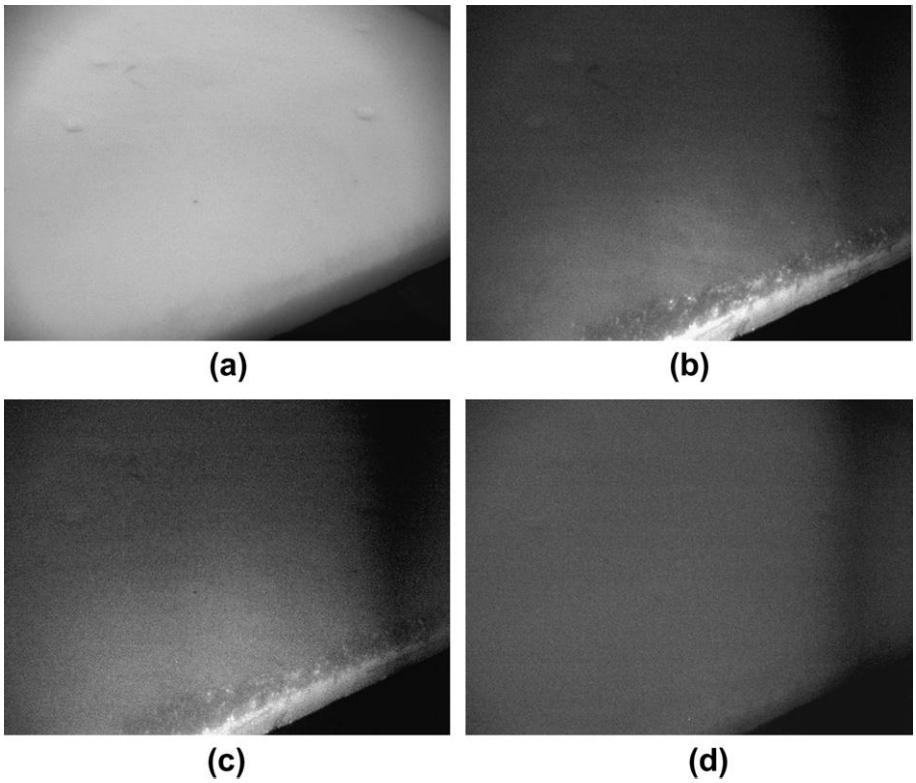

Fig. 7. White HDPE cutting board for fresh-cut vegetable products in Plant A. Digital photograph (a), images with violet LED illumination at 475 nm (b), 520 nm (c) and 675 nm (d) were acquired after cleaning and sanitation.

Table 2
ATP test results for vegetable cutting board shown in Fig. 7.

ATP test location	ATP result (RLU)
Cutting board over damaged fluorescent area	298,260
Cutting board over damaged fluorescent area	280,588
Nearby non-fluorescent area on cutting board	6532

3.2.2. HDPE and potential false positives

HDPE commonly shows a blue-green auto-fluorescence response to UV or violet excitation. In this study, accentuated auto-fluorescence-based responses appeared to be associated with physical damage to the surface. To examine the effect of some common sources of structural damage on fluorescence responses, HDPE coupons were deliberately damaged in the laboratory by sanding edges or by drilling holes (Fig. 9). Both sanded edges and drilled holes showed slightly enhanced fluorescence-based responses; however, relative increases in the fluorescence-based responses were much lower than the corresponding responses observed for the damaged areas of cutting board at Plants A and B. One possible explanation for these differences could be accumulation of fluorescent contaminants in the crevices of the damaged cutting boards in the processing plants.

In any case, as the results presented in the previous section suggest, damaged HDPE surfaces can serve as a reservoir for microorganisms. In response to the relatively high ATP readings that were found in Plant A along damaged HDPE edges, standard cleaning procedures were modified to include scrubbing edges with a stiff brush. During later visits, fluorescence-based responses in damaged areas were still seen at 475 and 520 nm, but ATP tests of these areas were reduced a 100-fold (one reading: 3050 RLU).

Some fluorescence responses of HDPE surfaces are unlikely to be related to a food safety issue. These responses appear to result from internal structural defects. In one example, several locations on a cutting board in Plant A were found to fluoresce at 520 nm; an ATP test of one such area measured 0 RLU, while tests of two non-fluorescent areas nearby yielded measurements of 1417 and 858 RLU (Fig. 10). Re-cleaning did not alter the fluorescence-based response at 520 nm. Similar results were found on other HDPE cutting boards, and the fluorescent responses due to these anomalies were often visible to the naked eye.

Most of these false positives can be identified with experience. Techniques that help identify the false positives include moving the camera around while viewing the anomaly, inspecting the area with the naked eye to look for signs of physical damage, re-cleaning and re-inspecting the area, and noting the area as a false positive for future inspections. If concerns remain, it would be appropriate to test for ATP.

3.3. Less well-defined examples

3.3.1. Blades

Images of cutting blades in Plant A revealed areas of possible contamination that repeatedly come in contact with the final product. At 675 nm, fluorescent debris was found on a rotating cutting blade indicative of plant debris stuck in a crevice where the blade attaches to the spindle (Fig. 11). Note the increased contrast in the difference image. In Fig. 12, similar results were observed on an apple slicer used for fresh-cut product. Test results showed relatively high ATP levels for the detected contamination site (Table 4). In both cases cleaning procedures were modified to improve overall cleanliness of the processing equipment.

What appeared to be mineral deposits were often seen in crevices in cutting implements, particularly at the junctions of the blades with the end-caps. No consistent pattern was observed with regard to ATP test results, and the deposits could not be removed

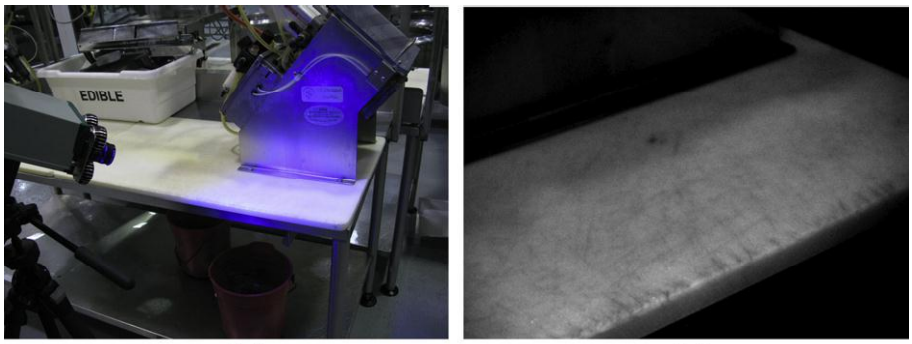

Fig. 8. White HDPE cutting board for fresh-cut vegetable products in Plant B. Digital photograph (a) and image with violet LED illumination at 475 nm (b) were acquired after cleaning and sanitation.

Table 3
ATP test results for HDPE surface shown in Fig. 8.

ATP test location	ATP result (RLU)
Edge of cutting board	16,719
Middle of cutting board	2356

by scrubbing. It is not clear whether this type of phenomenon represents a direct food safety concern. In any case, these crevices are difficult to clean and often accumulate produce residue, which is a food safety concern. These results suggest that there is room for improvement in protocols for cleaning blade structures.

3.3.2. Plastic curtain

Images of a clear plastic curtain used to separate processing areas in Plant A showed numerous fluorescence-based responses, many of which were visible to the naked eye (Fig. 13). The detected anomalies included some small brown masses that fluoresced at 520 nm. The masses had the appearance of a biofilm and it has been demonstrated that biofilms can be detected at 520 nm (Jun et al., 2009). Some green specs appeared to be residues from a nearby leafy greens processing area, and the specs could be detected at 675 nm. Unfortunately, this was an early visit and there were no materials available to perform more detailed tests. Furthermore, in response to the imaging results, the curtain was removed prior to the next visit.

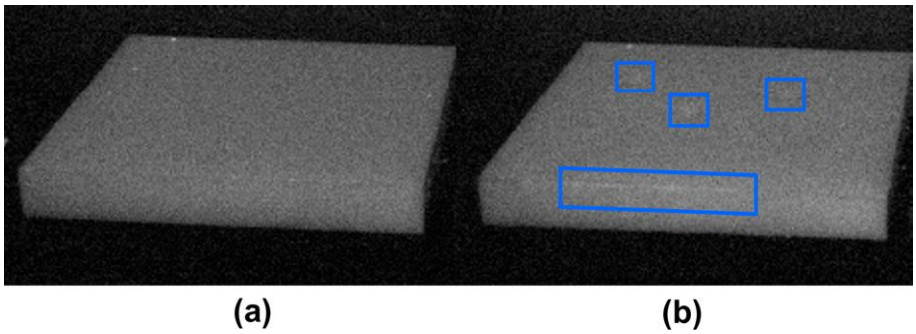

Fig. 9. HDPE coupon before (a) and after (b) simulated damage. Images were acquired at 475 nm and damage was done using a belt sander on the edge and by drilling three holes.

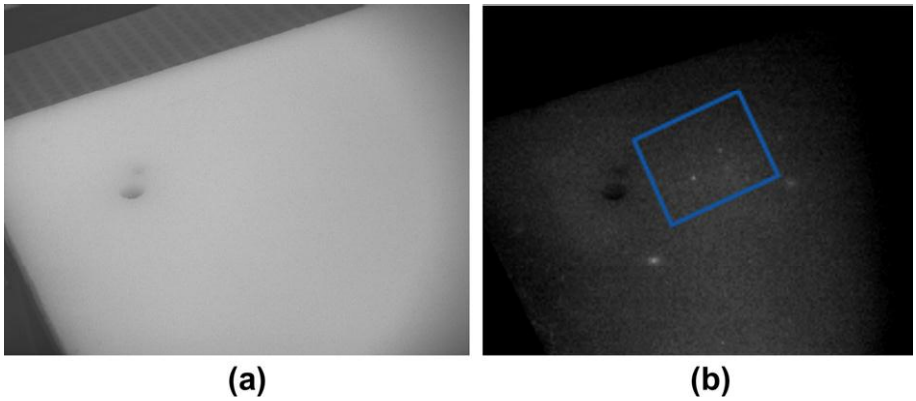

Fig. 10. Lettuce cutting board in Plant A. Images at 610 nm (a) and 520 nm (b) with violet LED illumination were acquired after cleaning and sanitation. Rectangle in (b) indicates area swabbed for initial ATP test.

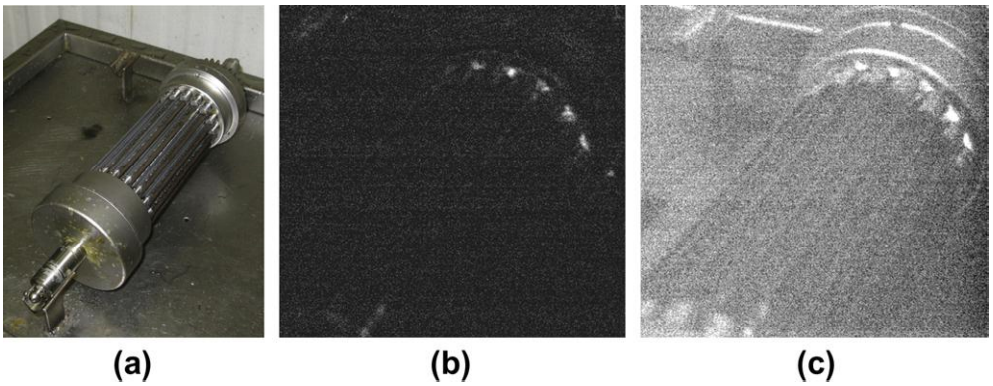

Fig. 11. Mechanical slicing blades in Plant A. Digital photograph (a), difference (b) and regular (c) images at 675 nm with LED illumination showing debris left in slicing equipment after cleaning and sanitation.

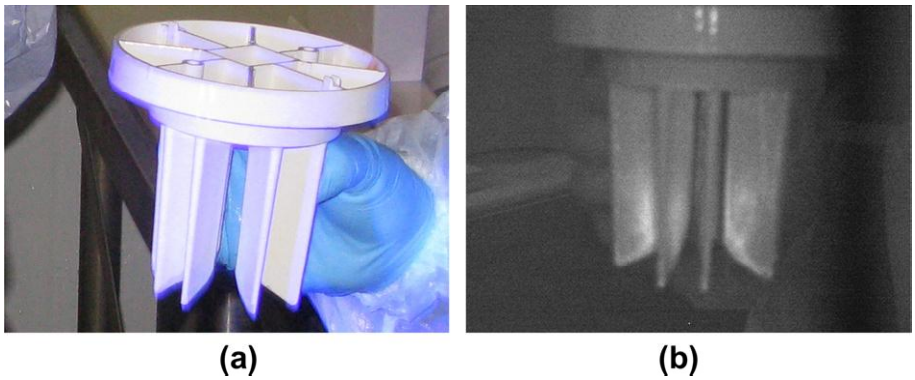

Fig. 12. Apple slicer in Plant A. Digital photograph (a) and image at 675 nm with LED illumination (b) reveal fluorescent contaminant left behind after cleaning and sanitation.

3.3.3. Pooled water

Refraction from pooled water (sanitizer) was detected as a fluorescence-based response at 520 nm (Fig. 14). An ATP test of the area measured 0 RLU while a test in an adjacent, non-fluorescent, area measured 1394 RLU. Changing the imaging angle changed the magnitude of the measured fluorescence-based response, and at some angles the response was essentially eliminated.

Table 4
ATP test results of apple slicer shown in Fig. 12.

ATP test location	ATP result (RLU)
Inside blade	8471
Top of blade holder	0

3.4. Practical considerations

3.4.1. Useful imaging system features

For Plants A and B, the three wavelengths selected for automated cycling, 475, 520, and 675 nm, allowed detection of all contaminants found in the two plants that evidenced fluorescence-based responses. These three wavelengths represent the overlap between spectral regions with relatively low ambient illumination resulting from the use of fluorescent lighting in the plants and fluorescence response spectra of potential targets of interest (Lefcourt et al., 2013). Many of the detected contaminants could not be seen at all three wavelengths. The ability to easily halt and restart cycling by tapping on the monitor image allowed for more in-depth screening using just one of the three cycling wavelengths. Imaging at 610 nm, an illumination intensity peak at both Plants A and B, with LED illumination turned off allowed the actual structure of a scene being imaged to be visualized; structural visualization was often, but not always, possible using one of the three selected cycling wavelengths.

A feature that was added following the first few visits to Plant A was the ability to automatically create a camera gain profile, where the profile represents a wavelength-dependent array of gains. This ability permitted the development of automatic cycling of imaging wavelengths, i.e., the profile matched the appropriate gain to the wavelength being used for imaging. To accommodate variations in image intensities resulting from differences in materials being imaged or ambient illumination intensity, this feature was expanded to allow display of a graph showing gain arrays by wavelength for five profiles and selection of one profile for use with two appropriate taps on the monitor screen (Lefcourt et al., 2013).

3.4.2. Value of hyperspectral imaging

The primary value of hyperspectral imaging concerns experimental use, i.e., to be able to search for unknown or unsuspected potential sources of contamination in a commercial environment. A secondary use is to identify the set of wavelengths to be used for detection. Generally, fluorescence imaging is a more sensitive detection method compared to reflectance imaging. The problem then becomes selection of the minimal set of wavelengths where ambient illumination is relatively low that will allow detection of all potential contaminates of interest. It is possible that this optimization function could be accomplished using a portable spectrophotometer or by switching among a set of band-pass interference filters. Either solution is practical as the scanning procedure would need to be done only once per facility unless a source of

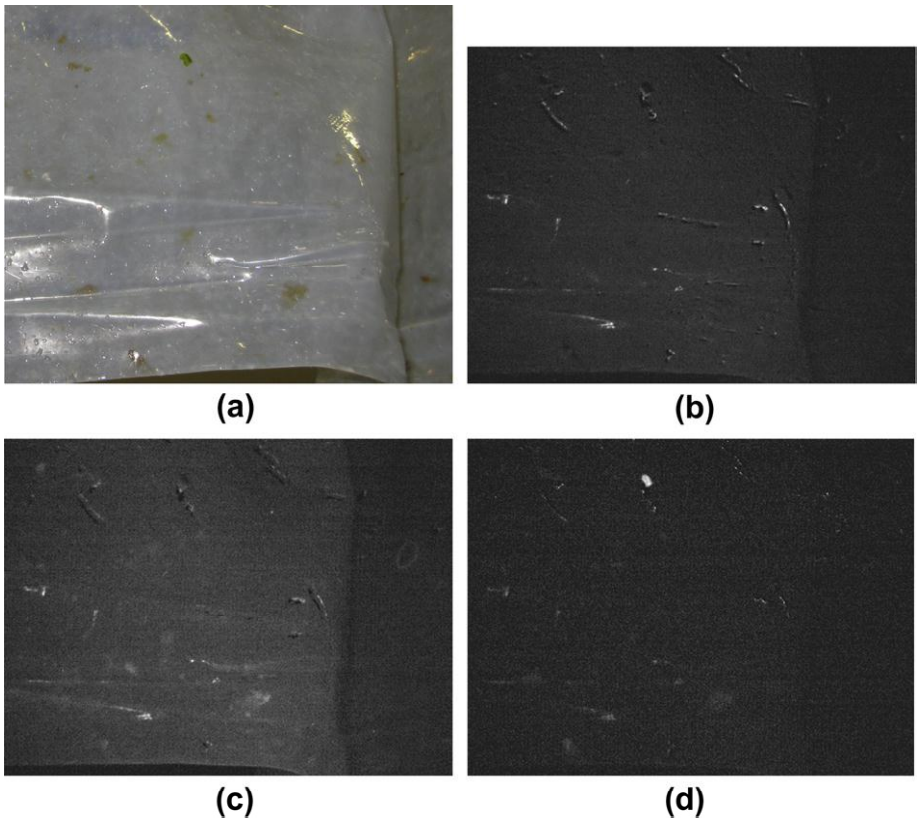

Fig. 13. Hanging plastic curtain in Plant A used to separate processing areas. Digital photograph (a), difference images at 420 nm (b), 530 nm (c) and 680 nm (d) were acquired after cleaning and sanitation. Difference images are presented to better highlight the unusually large number and variety of contaminants detected.

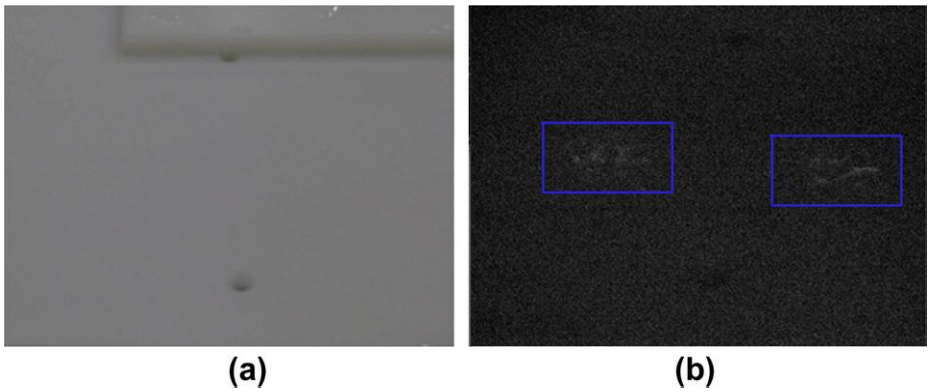

Fig. 14. Plastic cutting board for fresh-cut fruit in Plant A. Digital photograph (a) and image at 520 nm (b) were acquired after cleaning and sanitation. Boxes indicate locations of pooled water, which produced the measured response.

illumination changed. Alternatively, a portable hyperspectral system, such as the one used in this study, could be used for this initial survey.

Given the appropriate selection of wavebands for imaging, the question of how best to address differences in ambient illumination intensity by waveband would still remain. The simplest solution would be to use a camera that incorporates an automatic gain function. Automatic gain control is commonly available in relatively inexpensive cameras, whereas a camera where gain can be programmed is likely to be a more expensive camera. The cost advantage of a relatively inexpensive camera with automated gain control would have to be weighed against the decrease in sensitivity when imaging a scene that includes areas of relatively high and low intensity. In addition, when using an automated gain function, dwell time for cycling would have to be adjusted to allow the gain to stabilize.

3.4.3. Less useful imaging system features

As expected, difference images, i.e., subtraction of images without LED illumination from illuminated images by wavelength, did enhance contrast between fluorescent anomalies and background. In order to be able to acquire registered images with and without LED illumination, the current imaging system had to be mounted on the tripod. It is theoretically possible to eliminate the need for the tripod by increasing the camera frame rate for acquisition of sequential registered images with and without LED illumination. However, this would reduce the maximum potential exposure time and would probably require incorporation of some sort of

mechanism to address potential movement of the camera head. Such modifications would increase the cost and weight of the camera head. Testing of difference images was biased to some extent in that data needed to calculate difference images were only acquired once an anomaly was detected. Even so, no additional anomalies were detected in difference images.

Use of analytical procedures such as ratios of images acquired at two different wavelengths also requires acquisition of registered images, and is thus subject to some of the same constraints associated with difference images. One of the advantages of using image ratios is that ratios negate much of the effects of unequal fluorescence excitation intensity across the visual field of the camera (Kim et al., 2002). In contrast with difference images, it is possible to simultaneously acquire registered images at two wavelengths by using additional optics, and either halving the number of pixels in each of the two acquired images or using a second imaging array, e.g., CCD. However, results of this study indicate that ratio images are not essential for detecting anomalies of interest. This may be due in part to the natural tendency to center an anomaly of interest in the imaging field, thus negating any need or advantage for dealing with uneven excitation.

3.4.4. Human factors

A commercially-viable imaging system should not require a high level of expertise to use, be compact, and be inexpensive. The hyperspectral system requires a knowledgeable user, includes a backpack, and costs 15–20 thousand dollars to build. The laboratory has patented (Kim et al., 2012) and built a commercial handheld prototype that includes that ability to manually switch among three wavelengths; the cost of components is about 1000 dollars.

The questions remain as to who should use the unit, and how to get management and user acceptance. At both Plants A and B, interest in the imagining device grew over time. Three factors seemed to play a significant role in this increasing interest. First were the reports that were sent to companies after each visit. Second was the ability to highlight small particulates that had been missed during cleaning. Third was the ability to identify anomalies associated with high ATP readings. The net result was that, after a couple of visits, company personnel would often peer over the shoulder of the person handling the camera. In many cases, they would see something of concern and would try to immediately address the problem, usually by re-cleaning. In one case, the safety manager did not immediately believe the ATP results and insistent on re-testing using the company equipment. After re-testing and getting similar results, there was a noticeable increase in interest in the imaging system.

These experiences suggest that it would be appropriate to train the cleaning crew supervisor or a person from the safety staff in the use of the imaging device, and then to simply let them use it. Everyone we worked with was enthused about having a means to monitor the efficacy of cleaning efforts. Due to time constraints, it would not be practical to try to thoroughly inspect all cleaning efforts every day. However, in practice, it was found that concentrating on a single area on a given day led to improved cleaning protocols, and once the protocols were revised the identified problem was eliminated or greatly attenuated. A suggested imaging protocol might be to do a cursory survey of the entire processing area, and to do a detailed scan of a selected area. The area chosen for detailed inspection could be selected based on factors such as prior experience and a desire to provide a random check.

3.4.5. Analytical considerations

Given that a laptop computer is used by the hyperspectral system for image processing, consideration might be given to using this computational capability for additional image analysis. There are a number of techniques that have been developed for spatial analysis of individual images (Weeks, 1996) and techniques using both spatial and spectral data have been investigated for detecting contaminants on or problems with agricultural produce (Lefcourt et al., 2003; Kim et al., 2011). Additional image analysis could possibly provide a number of benefits, including: identification of objects of interest, improved contrast between targets and background, and reduction in the number of false positives. However, there are a number of constraints that limit the application of common analysis techniques. As targets generally have amorphous shapes, shape recognition techniques have limited applicability. As the VIS spectra of commodities likely to be of interest are broad and as there is considerable overlap across commodities (Wiederoder et al., 2012), identification of specific commodities would be difficult if not impossible. As discussed above, two techniques with demonstrated usefulness are taking the difference between images acquired with and without supplemental excitation illumination, and ratios of images acquired at different wavelengths. Edge detection is a technique that has been successfully used to highlight the location of target contaminants (Lefcourt et al., 2003; Fig. 15).

3.4.6. ATP findings

In agreement with recent observations by Lehto et al. (2011), ATP test results in this study indicate that theoretical hygiene goals in produce plants are not being met. Similarly, Cunningham et al. (2011) tested surfaces in retail food establishments after cleaning and found elevated ATP levels on most surfaces, e.g., average ATP readings for cutting boards exceeded 5000 RLU. They suggested that "the current practice of evaluating food contact surface cleanliness by sight and touch to meet regulatory requirements might

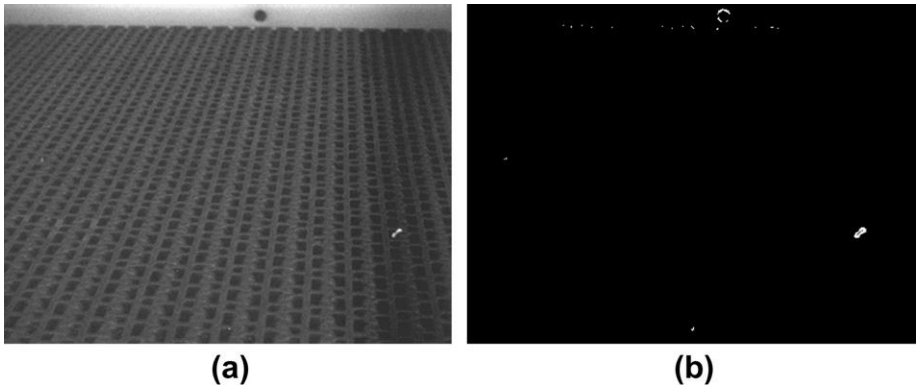

Fig. 15. Image of onion transport belt at 675 nm from Fig. 5 before (a) and after (b) edge detection using a 3 × 3 Sobel filter and thresholding (Lefcourt et al., 2003).

be inadequate." In this study, measured ATP levels were generally much higher than a suggested threshold of ~100 RLU. In many cases, changes made in cleaning protocols in response to imagining data resulted in dramatic decreases in measured ATP levels in problem areas. Even so, remediation seldom lowered ATP test results below the ~100 RLU threshold. The value of the imagining system in identifying problem areas is clear. Whether existing cleaning and sanitation measures can ever reduce most ATP test results in a fresh-cut processing plant to below ~100 RLU is less clear. It may be that this threshold is unrealistically stringent. Alternatively, it may be necessary to incorporate more aggressive cleaning measures, such as the use of steam, in hygiene plans.

4. Conclusion

Tests in commercial fresh-cut processing facilities demonstrated that the portable hyperspectral imaging system facilitated surface hygiene inspection following routine cleaning and sanitation. Imagining results provided real-time feedback to sanitation workers and resulted in efficacious changes in cleaning protocols. Detection of anomalies in the test facilities was facilitated by monitoring florescence-based responses to violet LED excitation while continuously cycling among three wavelengths; 475, 520, and 675 nm. Selection of wavelengths for detection was influenced by ambient lighting; the three wavelengths used correspond to troughs in the ambient lighting spectra at both test facilities. These results indicate that development of a consumer friendly fluorescence-based imaging system that incorporates the potential for imaging at multiple wavelengths is warranted, and that use of such a system is likely to reduce food safety risks. The device would have application anywhere food is processed, and could be employed by regulatory agencies and third party auditors to monitor or conduct inspections.

Acknowledgements

This work was funded by the USDA. Partial support for Michael S. Wiederoder and Nancy Liu was provided by the Department of Nutrition and Food Science, University of Maryland, College Park. The USDA is an equal opportunity employer.

References

Brody, S.S., 1958. New excited state of chlorophyll. Science 128 (3328), 838–839.
Chappelle, E.W., McMurtrey, J.E., Kim, M.S., 1991. Identification of the pigment responsible for the blue fluorescence band in the laser induced fluorescence (LIF) spectra of green plants, and the potential use of this band in remotely estimating rates of photosynthesis. Remote Sensing of Environment 36 (3), 213–218.
Cunningham, A.E., Rajagopal, R., Lauer, J., Allwood, P., 2011. Assessment of hygienic quality of surfaces in retail food service establishments based on microbial counts and real-time detection of ATP. Journal of Food Protection 74 (4), 686–690.
Donlan, R.M., Costerton, J.W., 2002. Biofilms: survival mechanisms of clinically relevant microorganisms. Clinical Microbiology Reviews 15 (2), 167–193.
Fatemi, P., Frank, J.F., 1999. Inactivation of Listeria monocytogenes/Pseudomonas biofilms by Peracid Sanitizers. Journal of Food Protection 62 (7), 761–765.
FDA, 2001. Analysis and evaluation of preventive control measures for the control and reduction/elimination of microbial hazards on fresh and fresh-cut produce. <http://www.fda.gov/Food/ScienceResearch/ResearchAreas/SafePracticesforFoodProcesses/ucm090977.htm> (accessed on 12.9.12).
FDA, 2008. Guidance for industry: guide to minimize microbial food safety hazards of fresh-cut fruits and vegetables. <http://www.fda.gov/food/guidancecomplianceregulatoryinformation/guidancedocuments/produceandplanproducts/ucm064458.htm> (Updated 2009 July 10; Accessed 12.9.12).
Fry, S.C., 1979. Phenolic components of the primary cell-wall and their possible role in hormonal-regulation of growth. Planta 146 (3), 343–351.
Fry, S.C., 1982. Phenolic components of the primary cell wall. Feruloylated disaccharides of D-galactose and L-arabinose from spinach polysaccharide. Biochemical Journal 203 (2), 493–504.
Hoffmann, S., Ficshbeck, P., Krupnici, A., McWilliams, M., 2007. Using expert ellicitation to link foodborne illnesses in the United States to foods. Journal of Food Protection 70 (5), 1220–1229.
Jun, W., Kim, M., Lee, K., Millner, P., Chao, K., 2009. Assessment of bacterial biofilm on stainless steel by hyperspectral fluorescence imaging. Sensing and Instrumentation for Food Quality and Safety 3 (1), 41–48.
Jun, W., Kim, M.S., Cho, B.-K., Millner, P.D., Chao, K., Chan, D.E., 2010. Microbial biofilm detection on food contact surfaces by macro-scale fluorescence imaging. Journal of Food Engineering 99 (3), 314–322.
Kim, M.S., Lefcourt, A.M., Chen, Y.R., Kim, I., Chan, D.E., Chao, K., 2002. Multispectral detection of fecal contamination on apples based on hyperspectral imagery: Part II. Application of hyperspectral fluorescence imaging. Transactions of the ASAE 45 (6), 2039–2047.
Kim, M.S., Chao, K., Chan, D.E., Yang, C., Lefcourt, A.M., Delwiche, S.R., 2011. Hyperspectral and multispectral imaging technique for food quality and safety inspection. In: Cho, Y., Kang, S. (Eds.), Emerging Technologies for Food Quality and Food Safety Inspection. CRC Press, New York, pp. 207–234.
Kim, M.S., Lefcourt, A.M., Chao, K., Chen, Y.R., Senecal, A.G., Marek, P., 2012. Handheld inspection tool and method. US patent number 8,310,544 B2.
Kumar, C.G., Anand, S.K., 1998. Significance of microbial biofilms in food industry: a review. International Journal of Food Microbiology 42 (1–2), 9–27.
Lammerding, A.M., Frazil, A., 2000. Hazard identification and exposure assessment for microbial food safety risk assessment. International Journal of Food Microbiology 58, 147–157.
Lefcourt, A.M., Kim, M.S., Chen, Y.R., 2003. Automated detection of fecal-contamination of apples by multispectral laser-induced fluorescence imaging. Applied Optics 42 (19), 3935–3943.
Lefcourt, A.M., Wiederoder, M.S., Liu, N., Kim, M.S., Lo, Y.M. 2013. Development of a portable hyperspectral imaging system for monitoring the efficacy of sanitation procedures in food processing facilities. Journal of Food Engineering. http://dx.doi.org/10.1016/j.jfoodeng.2013.01.043.
Lehto, M., Kuisma, R., Määttä, J., Kymäläinen, H.R., Mäki, M., 2011. Hygienic level and surface contamination in fresh-cut vegetable production plants. Food Control 22 (3), 469–475.
Lundquist, K., Josefsson, B., Nyquist, G., 1978. Analysis of lignin products by fluorescence spectroscopy. Holzforschung 32 (1), 27–32.
Pérez-Rodríguez, F., Valero, A., Carrasco, E., García, R.M., Zurera, G., 2008. Understanding and modelling bacterial transfer to foods: a review. Trends in Food Science & Technology 19 (3), 131–144.
Poulsen, L.V., 1999. Microbial biofilm in food processing. Lebensmittel-Wissenschaft und-Technologie 32 (6), 321–326.
Scallan, E., Griffin, P., Angulo, F., Tauxe, R., Hoekstra, R., 2011. Foodborne illness acquired in the United States – unspecified agents. Emerging Infectious Diseases 17 (7), 16–22.
Silagyi, K., Kim, S.H., Lo, Y.M., Wei, C.I., 2009. Production of biofilm and quorum sensing by Escherichia coli O157:H7 and its transfer from contact surfaces to meat, poultry, ready-to-eat deli, and produce products. Food Microbiology 26 (5), 514–519.
Weeks, A.R., 1996. Fundamentals of Electronic Image Processing. SPIE Optical Engineering Press, Seattle, WA.
Wiederoder, M.S., Lefcourt, A.M., Kim, M.S., Lo, Y.M., 2012. Detection of fresh-cut produce processing residues on food contact surface materials using hyperspectral imaging. Journal of Food Measurement and Characterization 6 (1–4), 48–55. http://dx.doi.org/10.1007/s11694-012-9132-1.